

THERMAL INFLUENCE OF COATINGS IN THE CUTTING TOOL LIFE

Rogério Fernandes Brito, rogbrito@unifei.edu.br

Sandro Metrevelle Marcondes de Lima e Silva, metrevel@unifei.edu.br

João Roberto Ferreira, jorofe@unifei.edu.br

Mechanical Engineering Institute - IEM, Federal University of Itajubá - UNIFEI, Prof. José Rodrigues Seabra campus, BPS Av., #1,303, Pinheirinho district, Zip code: 37500-903, Itajubá, MG, Brazil.

Solidônio Rodrigues de Carvalho, srcarvalho@mecanica.ufu.br

School of Mechanical Engineering - FEMEC, Federal University of Uberlândia - UFU, Santa Mônica campus, João Naves de Ávila Av., #2,160, Santa Mônica district, Zip code: 38400-902, Uberlândia, MG, Brazil.

Abstract. *The chip formation process may undergo plastic deformation during machining, where a high amount of heat is yielded. Heat is a parameter that plays an important role in the performance and lifespan of the tool. To improve the performance of the tool, several types of coatings are applied to its surface. These coatings are often ceramic materials that provide minor wear, with thermal isolation features. The temperature determination during the cutting is one of the most important factors in the study of the lifespan of tools because it enables the analysis and understanding of the wear mechanisms. This present work proposes a study of heat influence in diamond and K10 cemented carbide tools substrate considering the variation of the coating thickness. The coatings utilized in the present analysis were: titanium nitride coating (TiN) and aluminum oxide (Al₂O₃). The adopted coating thickness ranged from 1 to 10 (µm). The purpose of this thermal analysis is to investigate the thermal parameters involved in the analysis, enabling a better temperature distribution in the cutting zone aiming to increase the lifespan and reduce costs. The numerical methodology in this present work uses the ANSYS® CFX commercial package based on Finite Volume Method which obtains all the variables involved in the simulation at the same time interval. The calculations are carried out under transient regime. Boundary conditions by convection, heat flux besides the thermo physical properties of the tool and coating involved in the numerical analysis are known. To validate the proposed methodology an experiment under controlled conditions is used. The temperature field in the coated cutting tool as well as a thermal analysis of the coating influence are presented and discussed in the present study. We compare the results found here with those found in the literature.*

Keywords: *heat transfer, thermal analysis, finite volume method, cutting tool, coating.*

1. INTRODUCTION

A large amount of heat is generated in a machining process, as well as, in other processes in which deformation of the material occurs. Heat is a parameter that strongly influences the tool performance during this process. One way to increase the tool life consists of coating its cutting surface with materials that provide minor wear with thermal isolation features.

An important investigation consists of the study of the influence of cutting tool coatings on heat transfer and friction wear, resulting in a distribution of the cutting temperature both on the chip and on the tool. It may be observed in literature that most orthogonal metal cutting simulations were designed for uncoated cemented carbide tools and that now, an opposite trend has considered the use of single and multiple coatings. Some papers concerning coating studies are highlighted: In Marusich *et al.* (2002), the author carried out a simulation using a numerical model based on the Finite Element Method (FEM). The Thirdwave AdvantEdge® software was used to simulate the performance of chip-breakage of coated and uncoated tools. One of their results showed a temperature reduction of 100 (°C) for tool substrate with multi-layered coatings. Grzesik (2003) studied the cutting mechanisms of several coated cemented carbide tools. The study showed that, depending on the coating, the tool-chip contact area and the average temperature on the tool-work piece interface changed; however, it remained unproved whether the coatings were able to isolate the substrate. The first comprehensive study, addressing the assessment of an orthogonal cutting model, for multi-layer coated cemented carbide tools using the FEM was presented by Yen *et al.* (2003) and Yen *et al.* (2004). In this model, the thermal properties of three layers of titanium carbonate, (TiC), aluminum oxide (Al₂O₃) and titanium nitride (TiN) were analyzed, both individually and in group, considering a layer with equivalent thermal properties. The results indicated that the fine width coatings with an Al₂O₃ intermediary layer did not significantly alter the temperature gradients for a steady state between the chip and the tool substrate. Rech *et al.* (2004) and Rech *et al.* (2005) worked with the qualification of the tribological system 'work material - coated cemented carbide cutting tool - chip'. The objective of this study was to have a clearer understanding of the heat flux generated during the turning process. The application of the proposed methodology, for several coatings deposited on cemented carbide inserts, showed that the coatings did not have significant influence on the substrate thermal isolation. Kusiak *et al.* (2005) accomplished a study on the thermal influence of several coatings deposited on a cutting tool. This analysis was performed through an analytical model developed by the authors. An experimental test of AISI 1035 steel turning was carried out in order to

examine the different coated inserts for real cutting conditions. The results obtained showed that the Al_2O_3 coating presented a slight reduction on the tool heat flux while the other coatings used did not modify the thermal field significantly. Coelho *et al.* (2007) presented results on polycrystalline cubic boron nitride (PCBN) insert wear using the FEM. Titanium aluminum nitride (TiAlN) and aluminum chromium nitride (AlCrN), coated and uncoated cutting tools, were used in the turning of AISI 4340 steel. The simulations performed indicated that the temperature on the tool-chip interface was approximately 800 (°C) in the absence of flank wear, regardless of the coating.

The objective of the present work is to perform a numerical analysis of the thermal influence of the coating in cutting tools during the cutting process. The purpose of this analysis is to verify the thermal and geometrical parameters of the coated tool, focusing onto a more adequate temperature distribution in the cutting region. To obtain the cutting tool temperature field, the ANSYS® CFX Academic Research software v. 12 is used. The cutting tool used in the simulations of this present work has a single coating layer (Rech *et al.*, 2005).

In this work, ten cases with single layer coated cutting tools are analyzed, presenting varying thickness of 1 (μm) and 10 (μm) and two types of heat fluxes used on the tool-chip interface. They are: (1) 1 (μm) TiN coated K10 with uniform and time varying heat flux $q_1''(t)$; (2) 1 (μm) TiN coated K10 with heat flux $q_2''(t)$, where $q_2''(t) = 10 q_1''(t)$; (3) 10 (μm) TiN coated K10 with heat flux $q_1''(t)$; (4) 10 (μm) TiN coated K10 with heat flux $q_2''(t)$; (5) 1 (μm) TiN coated diamond with heat flux $q_2''(t)$; (6) 10 (μm) TiN coated diamond with heat flux $q_2''(t)$; (7) 1 (μm) Al_2O_3 coated K10 with flux $q_2''(t)$; (8) 10 (μm) Al_2O_3 coated K10 with flux $q_2''(t)$; (9) 1 (μm) Al_2O_3 coated diamond with flux $q_2''(t)$, and (10) 10 (μm) Al_2O_3 coated diamond with flux $q_2''(t)$.

Thus the temperature fields on the cutting tools are obtained, and a numerical analysis of the thermal influence of this coating is presented in this work.

2. PROBLEM DESCRIPTION

The thermal model of heat conduction and their regions for the imposition of the boundary conditions in three-dimensional coated tools are presented in Figs. 1a, 1b, and 1c. The geometry, with computational domain, represented respectively by Ω_1 and Ω_2 , the coating solids of height e , the cutting tool substrate of height H , and interface C between the coating and the substrate. Only one type of material was considered for the cutting tool bearing 12.7 (mm) x 12.7 (mm) x 4.7 (mm), with radius R of 0.8 (mm) and heat flux region S_2 with the area of approximately 1.424 (mm²). The coating width values adopted were: $e = 0.010$ (mm) and 0.001 (mm).

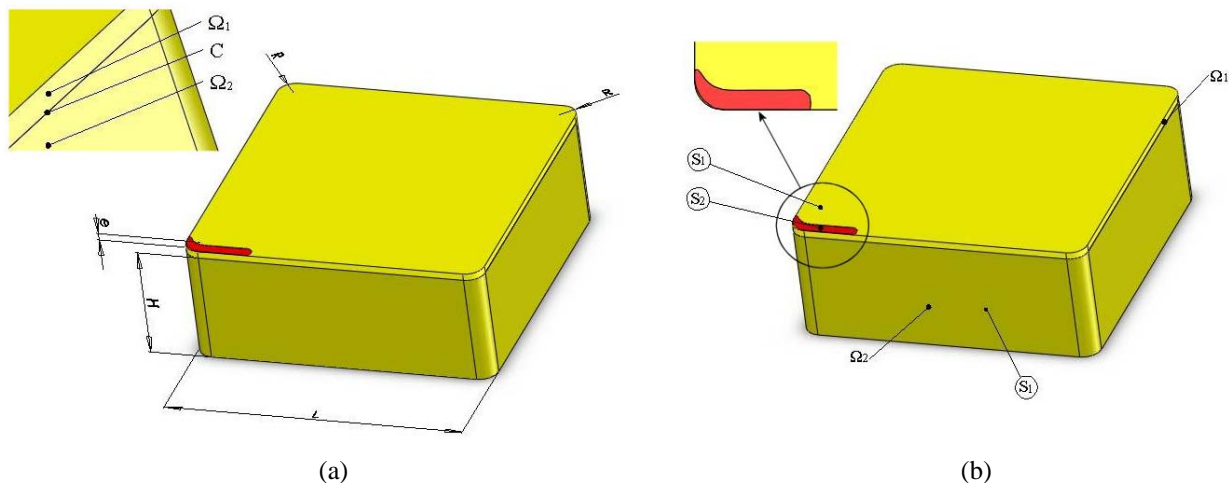


Figure 1. Coated cutting tool: interface detail (a) and the flux region (b).

The thermal parameters of the materials investigated, both the substrate and the tool coating, under ambient temperature were: K10 tool: $\rho = 14,900$ (kg m⁻³) [1], $C_p = 200$ (J kg⁻¹ K⁻¹) [3], $k = 130$ (W m⁻¹ K⁻¹) at 25 (°C) [1]; diamond tool: $\rho = 3,515$ (kg m⁻³) [4], $C_p = 471$ (J kg⁻¹ K⁻¹) [4], $k = 2,000$ (W m⁻¹ K⁻¹) [4]; TiN coating: $\rho = 4,650$ (kg m⁻³) [2], $C_p = 645$ (J kg⁻¹ K⁻¹) [2], $k = 21$ (W m⁻¹ K⁻¹) at 100 (°C) [2]; Al_2O_3 coating: $\rho = 3,780$ (kg m⁻³) [2], $C_p = 1,079$ (J kg⁻¹ K⁻¹) [2], $k = 28$ (W m⁻¹ K⁻¹) [2]. ([1] Engqvist *et al.*, 2000; [2] Yen *et al.*, 2004; [3] value adopted in the present work; [4] Matweb, 2009).

Figures 2a and 2b show one of the meshes used in the numerical simulation formed by hexahedral elements. Figure 2c shows a typical contact area on the tool-chip interface and the area used in the numerical simulation of the present work is, of an approximate value of 1.4245 (mm²). The area obtained in Carvalho (2005) for the following cutting conditions was: cutting speed of $v_c = 209.23$ (m/min), feed rate of $f = 0.138$ (mm/rot), and cutting depth of $p = 3.0$ (mm).

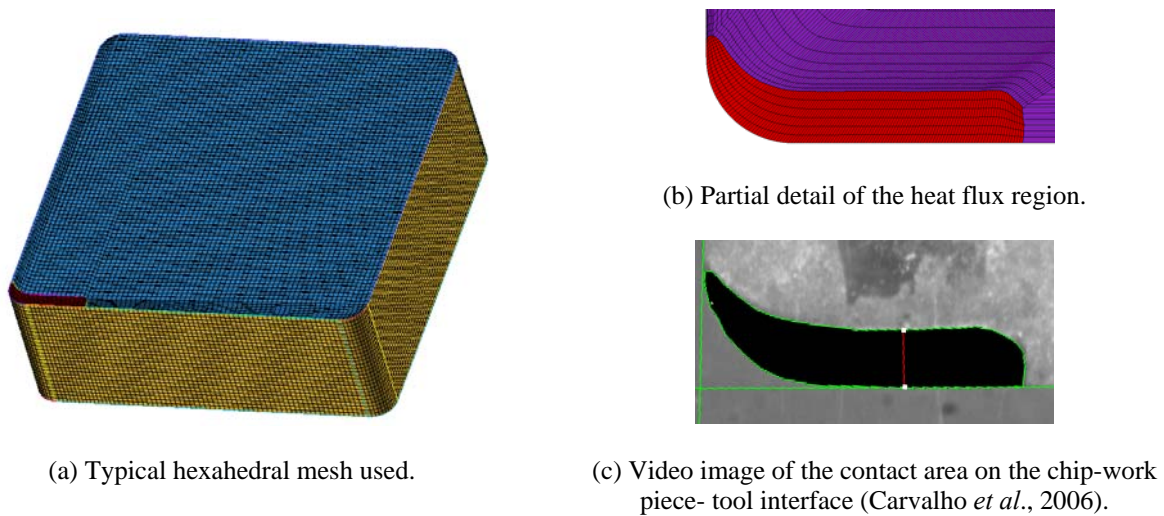


Figure 2. Non-structured finite volume mesh (a), mesh detail (b), image of the flux area (c).

2.1. Assumptions

The following hypotheses were considered in the present analysis: - three-dimensional geometrical domain; - transient regime; - absence of radiation models; - thermal properties, such as density ρ , thermal conductivity k , and specific heat capacity C_p are uniform and temperature independent for the coating layer and the substrate body; - there is a perfect thermal contact and no thermal resistance contact between the coating layer and the substrate body; - the boundary conditions of the heat flux $q''(t)$ are uniform and time variable; - the boundary conditions of the heat transfer coefficient h and room temperature T_∞ are constant and also known; - there is no internal heat generation, neither on the coating layer nor on the substrate body.

2.2. General implementation

Based on the considerations presented previously, the three-dimensional and transient heat diffusion equation is:

$$\left(\rho C_p\right)_i \frac{\partial T}{\partial t} = k_i \nabla^2(T), \quad (\text{in } \Omega_i, \text{ for } t > 0), \quad (1)$$

where $i = 1, 4$, with $i = 1$ for the TiN coating; $i = 2$ for the $K10$ cemented carbide cutting tool substrate; $i = 3$ for the Al_2O_3 coating, and $i = 4$ for the diamond substrate cutting tool.

The heat diffusion equation is subject to two types of boundary conditions: imposed time-varying heat flux in S_2 and constant convection in S_1 of the cutting tool. The initial temperature conditions are described for the thermal states of the substrate and coating solids as $T_i = 29.5$ (°C).

3. NUMERICAL METHOD

The solution of the continuity, momentum, and energy equations uses the Fluid Dynamics Calculus using the Finite Volume Method (*FVM*) with Eulerian scheme for the spatial and temporal discretization of the physical domain, using a finite number of control volumes (Versteeg and Malalasekera, 2007; Löhner, 2008).

Through this method, the control volume elements follow the Eulerian scheme with unstructured mesh (Barth and Ohlberger, 2004). Through this scheme, the transport equations may be integrated by applying Gauss Divergence Theorem, where the approximation of surface integral is done with two levels of approximation: first, the physical variables are integrated in one or more points on the control volume faces; second, the integrating value in the centered faces is approximated in terms of nodal values. This approximation by the nodal value in the control volume centered faces represents the average physical quantity in all the control volume with second order accuracy (Shaw, 1992).

More details on the concepts involved by the *FVM* may be found in Barth and Ohlberger (2004) where the discretization techniques, integral approximation techniques, convergence criteria and calculus stability are explored.

4. NUMERICAL VALIDATION

Figure 3 shows a study on the influence of mesh refinement on the temperature results, calculated in this present work with the use of the ANSYS® CFX Academic Research software, v. 12. The analysis of the numerical mesh convergence was done by using the following thermal properties of the *ISO K10* 12.7 (mm) x 12.7 (mm) x 4.7 (mm) cemented carbide cutting tool (Fig. 5a): $k = 43.1$ ($\text{W m}^{-1} \text{K}^{-1}$), $C_p = 332.94$ ($\text{J kg}^{-1} \text{K}^{-1}$) and $\rho = 14,900$ (kg m^{-3}). The convergence test analyzed different dimension meshes and their influence on the temperatures calculated by the numerical model was verified. The temperature was calculated for points $x = 6.35$ (mm), $y = 6.35$ (mm), and $z = 4.7$ (mm) on the cutting tool shown in Fig. 5a.

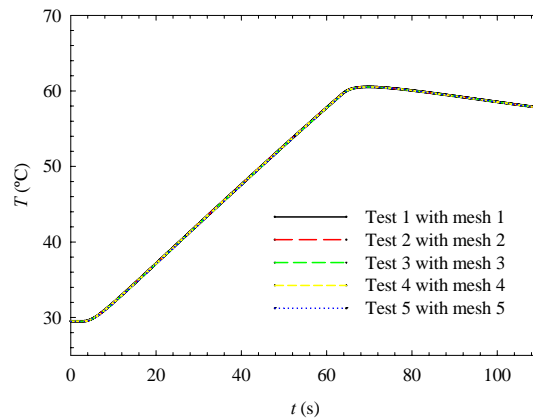


Figure 3. Comparison of the temperatures calculated for the different meshes presented on Tab. (2).

Table 1 shows the dimensions of the hexahedral forms of each element and the number of nodal points (*NP*) and of (*NE*) elements used in each convergence test. The following parameters were used in all mesh tests: time interval of 0.22 (s), equal initial and room temperature at 29.5 (°C), constant and equal heat transfer coefficient at 20 ($\text{W m}^{-2} \text{K}^{-1}$), total time of 110 (s), and area subjected to heat flux of 108.16 (mm^2).

Table 1. Numbers of nodal points and elements for each mesh test studied.

Test	Refinement (x, y, z) in (mm)	<i>NE</i>	<i>NP</i>
1	2.0 x 2.0 x 0.8	216	343
2	1.0 x 1.0 x 0.4	1,728	2,197
3	0.5 x 0.5 x 0.2	14,196	16,038
4	0.25 x 0.25 x 0.1	122,200	129,744
5	0.125 x 0.125 x 0.05	958,894	988,380

According to this study (Fig. 3), it seems clear that there was little difference as to the calculated temperature values. Moreover, the temperature residue among the meshes is practically negligible, with a deviation among them of less than 1 % for all the simulated time range. We can conclude that Test 3 mesh is enough to obtain good accuracy and low cost computational time results. For a mesh developed with a greater number of elements than those used in Test 5, the temperature value barely varies with mesh refinement.

The present work utilizes the experimental and numerical results from Carvalho (2005) and Carvalho *et al.* (2006) in order to make a comparison with results obtained with the use of the software utilized for this present work. Carvalho (2005) carried out an experiment under controlled conditions in which an *ISO K10* 12.7 (mm) x 12.7 (mm) x 4.7 (mm) cemented carbide cutting tool was used (Fig. 5a). Figure 4 shows the experimental thermal flux delivered to the cutting tool (Fig. 4a) and the temperatures measured by two thermocouples (Fig. 4b) for time varying from $t = 0$ to 110 (s). The thermocouples were embedded in the cutting tool (Fig. 5a) on the following positions: thermocouple T_1 : $x = 4.3$ (mm); $y = 3.5$ (mm); $z = 4.7$ (mm) and thermocouple T_2 : $x = 3.5$ (mm); $y = 8.9$ (mm); $z = 4.7$ (mm).

The data from this experiment are used as input data for the numerical validation of the ANSYS® CFX Academic Research software, v. 12 used in this present work. In this numerical model validation, the cutting tool, numerically simulated thermal properties, were: $k = 43.1$ ($\text{W m}^{-1} \text{K}^{-1}$), $C_p = 332.94$ ($\text{J kg}^{-1} \text{K}^{-1}$) and $\rho = 14,900$ (kg m^{-3}). The coordinates x, y, z of each thermocouple T_1 and T_2 (Fig. 4b) were measured for the comparison between the experimentally measured temperatures and those simulated by the ANSYS® Academic Research, v. 12.

Figure 5 shows the geometry (Fig. 5a) and the mesh (Fig. 5b) generated and used in the present work for the numerical validation of the ANSYS® CFX Academic Research software, v. 12. The numerical mesh was developed

with the help of ANSYS® ICEM-CFD, part of ANSYS® CFX Academic Research software, v. 12. It can be verified from Fig. 5b that the ANSYS® ICEM-CFD software generated a, three-dimensional structured mesh, in which the regions in blue and green represent the cutting tool, and the green region is the area (Fig. 5b) subjected to the heat transfer rate obtained experimentally by Carvalho (2005) (Fig. 8b). Following the study on the mesh independence (Tab. 1), a three-dimensional mesh containing 15,548 hexahedral elements and 17,497 nodal points was used. The green area is 10.4 (mm) x 10.4 (mm), on the xy -plane for $z = 0$ (mm). Once the mesh is generated, the implementation process for the boundary and initial conditions are started on ANSYS® CFX-Pre. To solve the problem, the ANSYS® CFX-Solver (ANSYS, Inc., 2008) is used. In the numerical test preparation on the ANSYS® CFX Academic Research software, v. 12, temperature monitoring points were inserted during the numerical simulation of this present work, equivalent to the positions of the thermocouples T_1 and T_2 inserted in the tool during the experiment carried out by Carvalho (2005).

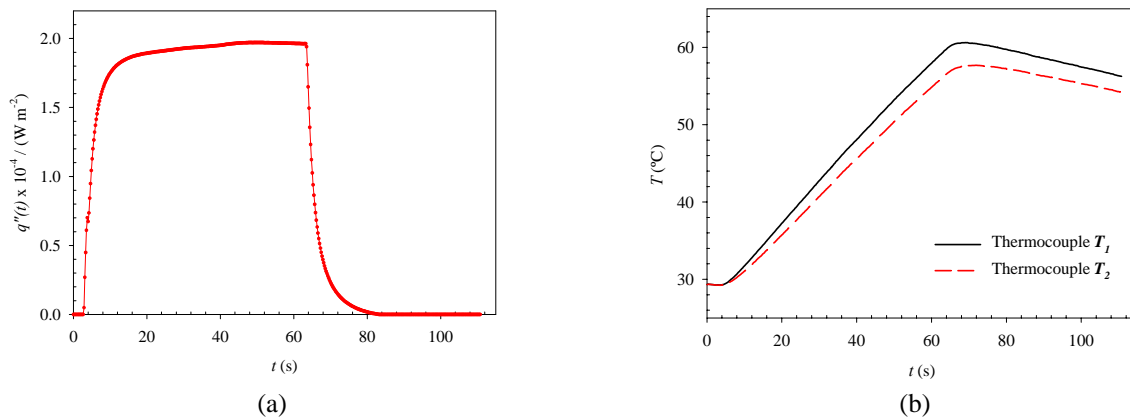


Figure 4. Experimental thermal flux (a) (Carvalho, 2005), and experimental temperature (b) (Carvalho, 2005).

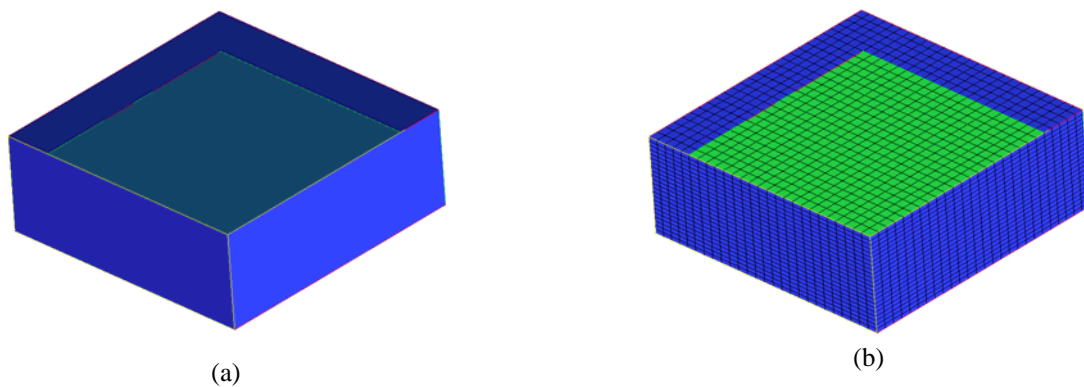


Figure 5. Geometry (a) and Three-dimensional mesh (b).

Figures 6a and 6b show a comparison between the temperatures obtained experimentally and numerically from thermocouples T_1 and T_2 by Carvalho (2005) and the temperatures obtained numerically in this present work with the ANSYS® CFX Academic Research software, v. 12. The largest and the smallest deviation found in relation to Carvalho's experimental case (Carvalho, 2005) was respectively 6.07 % for thermocouple T_2 and -0.53 % also for thermocouple T_2 . The largest and the smallest deviation found in relation to Carvalho's numerical case (Carvalho, 2005) was respectively -2.18 % for thermocouple T_2 and 0.25 % also for thermocouple T_2 .

It was verified that, with the numerical simulations done in the present Test (Fig. 6), the highest temperature gradients on the cutting tool occurred for the time instant of approximately 67 (s), reaching temperature values of approximately 79 (°C). From instant 63 (s), the heat flux starts a dropping process where temperature starts falling after approximately 4 (s). It may be observed that the blue region on the tool (Fig. 5b) is not in physical contact with any metal except with the environment. This situation, at room temperature $T_\infty = 29.2$ (°C) and with heat transfer coefficient $h = 20$ ($\text{W m}^{-2} \text{K}^{-1}$) (Yen *et al.*, 2003), considerably favored, the heat transfer rate dissipation on the tool causing the temperature to fall from approximately 79 (°C) to 71.6 (°C) at final instant 110 (s).

Following the validation with the numerical and experimental data from Carvalho (2005) and Carvalho *et al.* (2006), the thermal model and the numerical solution for the machining process, proposed in the present work using Sandvik® Coromant ISO K10 cemented carbide and diamond tools, are concluded. Thus, the numerical models for TiN and Al_2O_3

cutting tools are implemented in the present work, varying the thickness and the heat flux value imposed on the cutting tool. The heat rate $q(t)$ (Fig. 8a), obtained experimentally as in Carvalho (2005) and used in the validation in item 4 of the present work, was used to obtain the results for this present work.

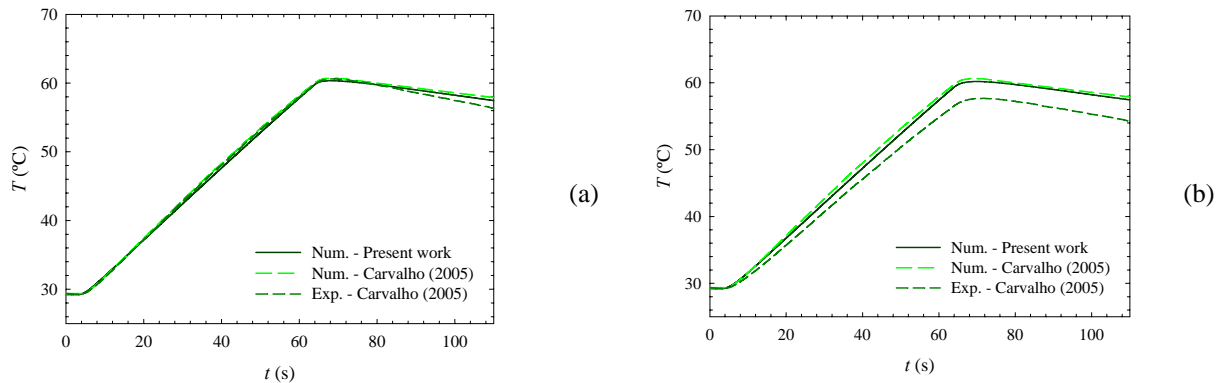


Figure 6. Thermocouples T_1 (a) and T_2 (b): comparisons between the numerical and experimental temperatures (Carvalho, 2005) and that calculated numerically in the present work.

The results obtained numerically in the thermal simulation of $K10$ type TiN and Al_2O_3 coated cemented carbide and diamond cutting tools are presented next. It is highlighted that the cemented carbide tool used in this simulation possesses different thermal conductivity from that used in item 4.

5. RESULT ANALYSIS

In order to investigate the temperature distribution for a time interval t , ten cases were selected. The main objective is to analyze the thermal influence of the heat flux and the thickness variation of coated cutting tools.

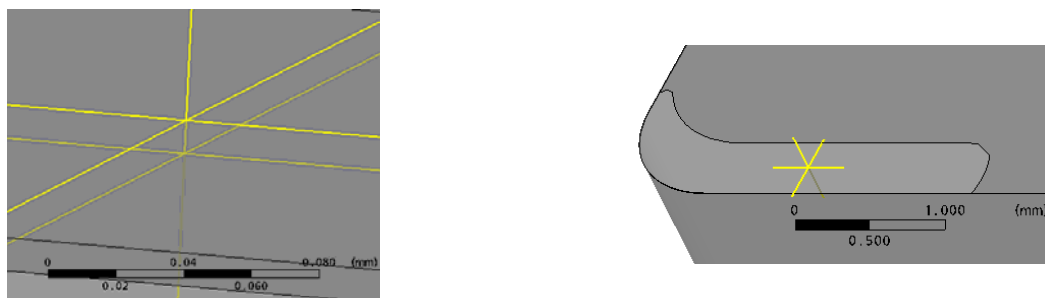
Table 2 shows temperature values obtained on the chip-tool and the coating-substrate interfaces, at instant 63 (s), calculated in the present work with the use of the ANSYS[®] CFX Academic Research software, v. 12. For the 1 (μm) coating with flux $q_2''(t)$, the highest and the lowest calculated temperature difference was for Case 2 (TiN coated $K10$ substrate) and for Case 9 (Al_2O_3 coated diamond substrate), respectively. For 10 (μm) coating with flux $q_2''(t)$, the highest and lowest calculated temperature difference was for Case 4 (TiN coated $K10$ substrate) and Case 8 (Al_2O_3 coated $K10$ substrate), respectively.

Table 2. Numerical results obtained from the temperature values at instant 63 (s).

Case	Coating (μm)	Variable heat flux (W m^{-2})	Temperature on Chip-Tool interface T_{CT} ($^{\circ}\text{C}$)	Temperature on Coating-Substrate interface T_{CS} ($^{\circ}\text{C}$)	Temperature Difference $T_{CT} - T_{CS}$ ($^{\circ}\text{C}$)
1	1	$q_1''(t)$	86.56	86.38	0.19
2	1	$q_2''(t)$	600.15	598.29	1.86
3	10	$q_1''(t)$	87.12	86.30	0.82
4	10	$q_2''(t)$	605.80	597.60	8.20
5	1	$q_2''(t)$	790.25	789.75	0.50
6	10	$q_2''(t)$	795.65	788.45	7.20
7	1	$q_2''(t)$	599.71	599.34	0.37
8	10	$q_2''(t)$	603.33	598.03	5.29
9	1	$q_2''(t)$	790.05	789.75	0.30
10	10	$q_2''(t)$	793.25	787.95	5.30

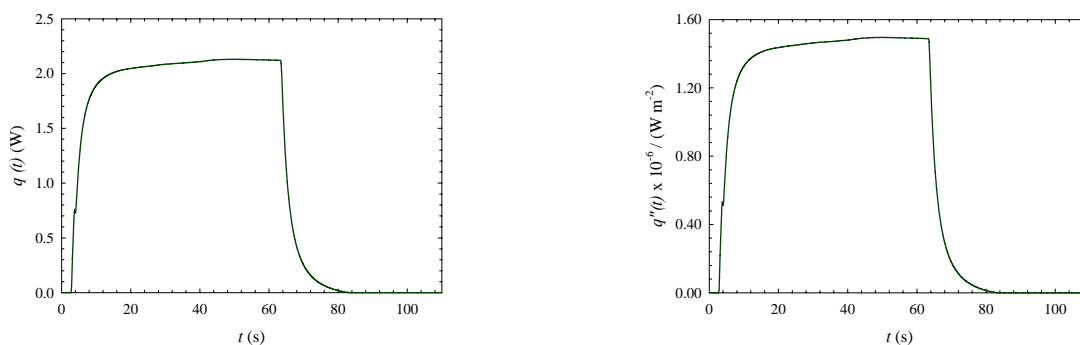
Figure 7 shows the two temperature monitoring points during the numerical simulations carried out in this present work. For the coordinates on the tool substrate-coating interface: $x = 1.5$ (mm), $y = 0.25$ (mm), and $z = 10$ (μm) and on the coating: $x = 1.5$ (mm), $y = 0.25$ (mm) and $z = 0$ (mm).

Figures 8a and 8b show the heat rate $q(t)$ (W) and the heat flux $q_1''(t)$ (W m^{-2}), respectively, varying in time used in this present work.



(a) Detail of the two temperature monitoring points. (b) Position of the temperature monitoring.

Figure 7. Temperature monitoring points located on and under the 10 (μm) TiN coating layer, using the ANSYS® CFX-Pre, included in the ANSYS® CFX Academic Research software, v. 12.



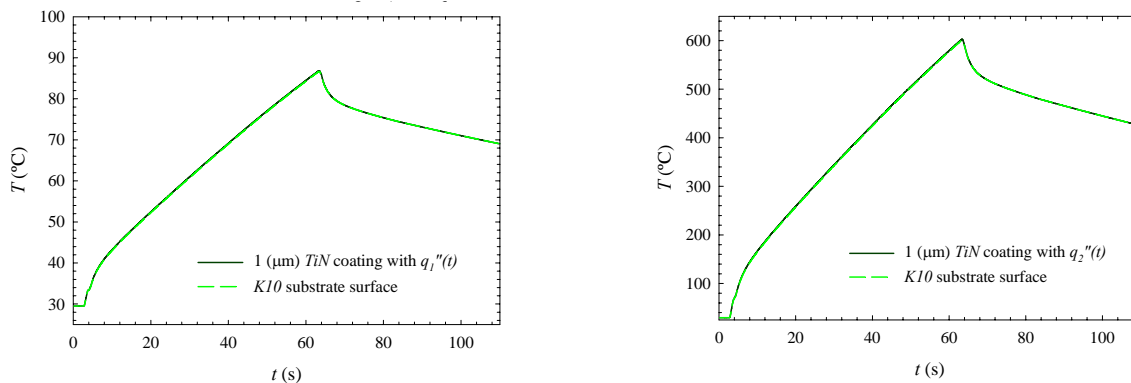
(a) Heat rate $q(t)$ (Carvalho, 2005).

(b) Heat flux $q_1''(t)$.

Figure 8. Heat rate and heat flux utilized in the present work.

Figures 9 to 13 show the simulation results with coated cutting tools carried out in the present work. The influence of the heat flux and coating thickness variation on the temperature fields on the chip-tool coating-substrate interfaces can be verified in these figures. It can be observed that the coating did not influence the temperature reduction, resulting, as a consequence into a small influence on the thermal isolation. The greater temperature decrease happened in Case 04 (Fig. 10b and Tab. 3), with thickness of 10 (μm), where the temperature value decreased from 605.80 (°C) to 597.60 (°C), at instant 63 (s), resulting in a value of 8.20 (°C).

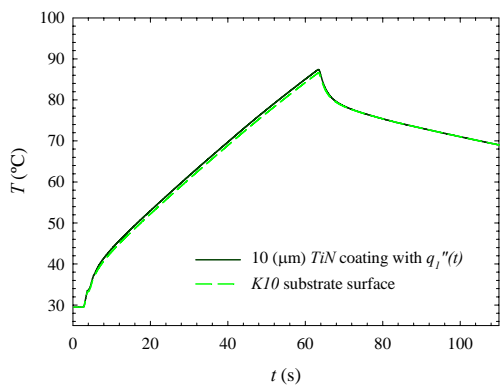
In most of the simulated cases, the number of nodal points was 501,768 and the number of hexahedral elements was 481,500.



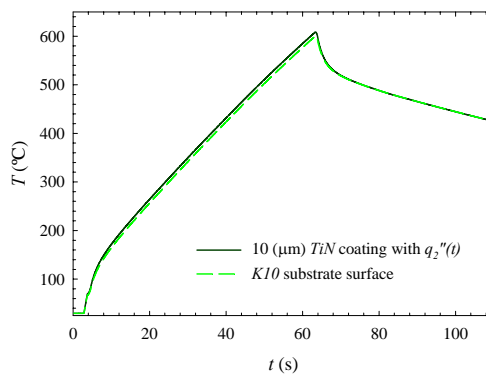
(a) Heat flux $q_1''(t)$.

(b) Heat flux $q_2''(t)$.

Figure 9. Cases 01 (a) and 02 (b) – Influence of the heat flux variation on the temperature - K10 substrate TiN coating.

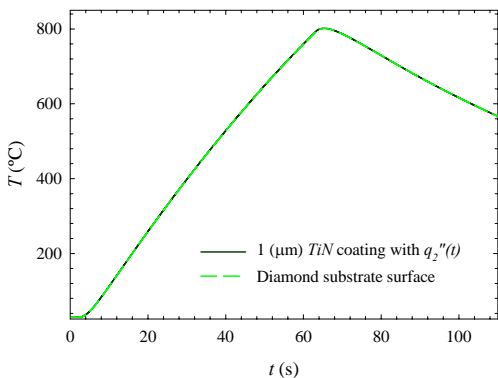


(a) Heat flux $q_1''(t)$.

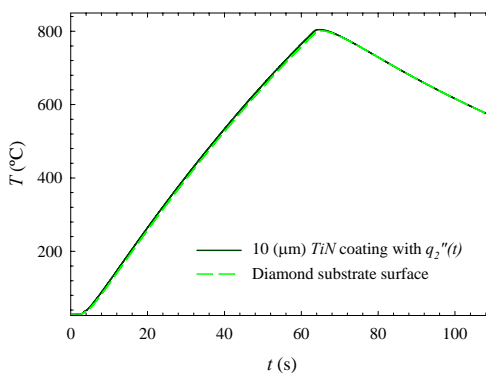


(b) Heat flux $q_2''(t)$.

Figure 10. Cases 03 (a) and 04 (b) – Influence of the heat flux variation on the temperature - *K10* substrate and *TiN* coating.

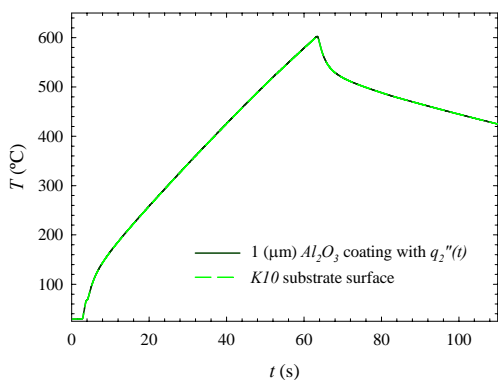


(a) 1 (μm) coating.

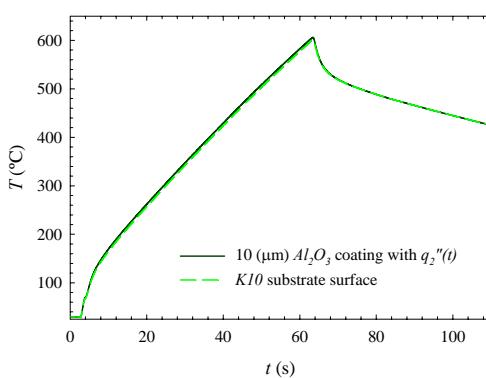


(b) 10 (μm) coating.

Figure 11. Cases 05 (a) and 06 (b) – Influence of the coating thickness variation on the temperature - diamond substrate and *TiN* coating.

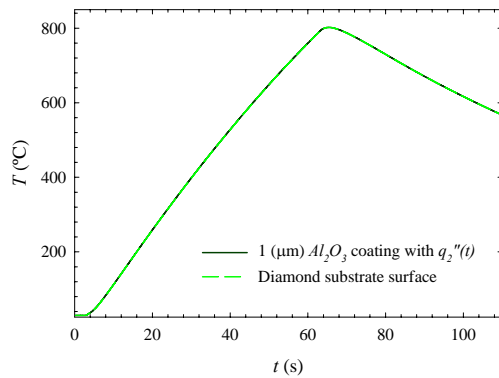


(a) 1 (μm) coating.

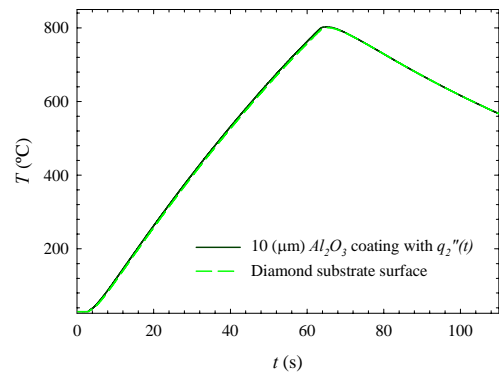


(b) 10 (μm) coating.

Figure 12. Cases 07 (a) and 08 (b) – Influence of the coating thickness variation on the temperature - *K10* substrate and Al_2O_3 coating.



(a) 1 (μm) coating.



(b) 10 (μm) coating.

Figure 13. Cases 09 (a) and 10 (b) – Influence of the coating thickness variation on the temperature – diamond substrate and Al_2O_3 coating.

Figures (14a), (14b), and (14c) show the temperature fields at instant 63 (s), top, bottom, and the heat flux surface views through isotherms for Case 4 of $K10$ cemented carbide substrate tool with 10 (μm) TiN coating.

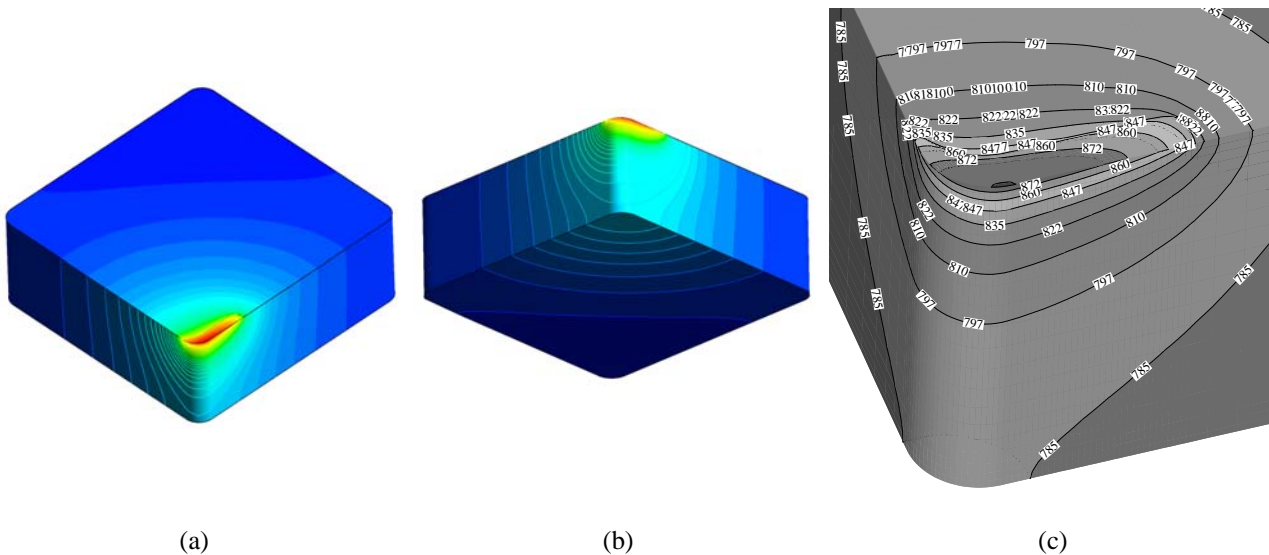


Figure 14. Top (a), bottom (b), and the heat flux surface (c) views of the temperature fields measured in (K), on the $K10$ TiN coated cutting tool for Case 4, at instant $t = 63$ (s).

One of the contributions of this work is the development of a numerical methodology which permits the simulations of complex form geometries, as well as, the inclusion of a more realistic heat flux in relation to the experimental case.

The implemented numerical methodology, along with the use of commercial software and CAD tools, may be applied in the simulation of heat transfer in complex geometry cutting tools. It may be observed from Fig. 14 that the heat flux region has an area as close as possible to the experimental (Fig. 2c) (Carvalho, 2005 and Carvalho *et al.*, 2006) and numerical areas of the heat flux, where a simple rectangular numerical area was adopted (Carvalho, 2005). The heat flux area used in this work (Fig. 2b) was obtained from the area measured on the tool (Fig. 2c) in an experiment carried out as in Carvalho (2005).

6. CONCLUSIONS

The following conclusions may be cited regarding the numerical results obtained for the thermal model of heat transfer in coated cutting tools: i - the studies carried out during the execution of the work showed that for a uniform heat source varying in time, considering a constant contact surface on the chip-tool, the temperature on the tool may be slightly influenced by the coatings when the thermal properties of the coating are very different from those of the substrate, even for fine 1 (μm) coating; ii - by increasing ten times the heat flux imposed on the chip-tool interface, a proportional increase of approximately seventeen times was caused in the difference of the temperatures measured at

the monitoring points (Case 10). iii - the coating deposited on the analyzed cemented carbide tool did not show satisfying results during a continuous cutting process. It showed a slight reduction in the heat flux for the cases studied in (Yen *et al.*, 2004; Rech *et al.*, 2004; Rech *et al.*, 2005; Kusiak *et al.*, 2005; Coelho *et al.*, 2007); iv - for the 1 (μm) TiN coating, there was no significant change on the heat flux penetrating the cemented carbide tool substrate; v - the present heat transfer analysis in coated cemented carbide cutting tools, using computational tools, revealed promising features in the study of the tool life, cost reduction in dry machining processes, lowering the time spent on the study of thermal influence of coatings, and reduction of experiments with the use of commercial computational tools; and vi - a more detailed investigation is necessary in order to include other types of coating materials, their thickness, considering the influence of temperature variation on the thermal conductivity k and specific heat capacity C_p .

7. ACKNOWLEDGEMENTS

The authors would like to thank The Research Support Foundation of the State of Minas Gerais (*FAPEMIG*), The Scientific Community Support Fund (*CAPES*), and The National Council for Research and Development (*CNPq*) for the financial support granted for the present work, as well as Engineering Simulation and Scientific Software (*ESSS*) company for the technical support in use of the ANSYS® CFX Academic Research software v. 12.

8. REFERENCES

- ANSYS, Inc., 2009, "ANSYS® CFX Academic Research Software, Release 12.0, Help System, Coupled Field Analysis Guide".
- Barth, T. and Ohlberger, M., 2004, "Finite Volume Methods: Foundation and Analysis, Encyclopedia of Computational Mechanics", Ed. Wiley, 57 p.
- Carvalho, S.R., 2005, "Determining the Temperature Field in Cutting Tools during a Turning Process", Ph.D. thesis, Federal University of Uberlândia, Uberlândia, Brazil.
- Carvalho, S.R., Lima e Silva, S.M.M., Machado, A.R. and Guimarães, G., 2006, "Temperature Determination at the Chip-Tool Interface using an Inverse Thermal Model considering the Tool and Tool Holder", Journal of Materials Processing Technology, Vol. 179, pp. 97-104.
- Coelho, R.T., Ng, E.G. and Elbestawi, M.A., 2007, "Tool Wear when Turning Hardened AISI 4340 with Coated PCBN Tools using Finishing Cutting Conditions", International Journal of Machine Tools and Manufacture, Vol. 47, pp. 263-272.
- Engqvist, H., Hogberg, H., Botton, G.A. Ederyd, S. and Axén, N., 2000, "Tribofilm Formation on Cemented Carbides in Dry Sliding Conformal Contact", Wear, Vol. 239, pp. 219-228.
- Grzesik, W., 2003, "A Computational Approach to Evaluate Temperature and Heat Partition in Machining with Multiplayer Coated Tools", International Journal of Machine Tools and Manufacture, Vol. 43, pp. 1311-1317.
- Kusiak, A., Battaglia, J.L. and Rech, J., 2005, "Tool Coatings Influence on the Heat Transfer in the Tool during Machining", Surface and Coatings Technology, Vol. 195, pp. 29-40.
- Löhner, R., 2008, "Applied Computational Fluid Dynamics Techniques: an Introduction based on Finite Element Methods", Second ed., Ed. Wiley, 544 p.
- Marusich, T.D., Brand, C.J. and Thiele, J.D., 2002, "A Methodology for Simulation of Chip Breakage in Turning Processes using an Orthogonal Finite Element Model", Proceedings of the Fifth CIRP International Workshop on Modeling of Machining Operation, West Lafayette, USA, pp. 139-148.
- Matweb, 2009, <http://www.matweb.com>.
- Rech, J., Battaglia, J.L. and Moisan, A., 2005, "Thermal Influence of Cutting Tool Coatings", Journal of Materials Processing Technology, Vol. 159, pp. 119-124.
- Rech, J., Kusiak, A. and Battaglia, J.L., 2004, "Tribological and Thermal Functions of Cutting Tool Coatings", Surface and Coatings Technology, Vol. 186, pp. 364-371.
- Shaw, C.T., 1992, "Using Computational Fluid Dynamics - An Introduction to the Practical Aspects of using CFD", Ed. Prentice Hall Publications.
- Versteeg, H. and Malalasekera, W., 2007, "An Introduction to Computational Fluid Dynamics: the Finite Volume Method", Second ed., Ed. Prentice Hall, 520 p.
- Yen, Y.C., Jain, A., Chigurupati, P., Wu, W.T. and Altan, T., 2003, "Computer Simulation of Orthogonal Cutting using a Tool with Multiple Coatings", Proceedings of the Sixth CIRP International Workshop on Modeling of Machining Operation, McMaster University, Canada, pp. 119-130.
- Yen, Y.C., Jain, A., Chigurupati, P., Wu, W.T. and Altan, T., 2004, "Computer Simulation of Orthogonal Cutting using a Tool with Multiple Coatings", Machining Science and Technology, Vol. 8, pp. 305-326.

9. RESPONSIBILITY NOTICE

The authors are solely responsible for the content of the printed material included in their work.